

LABORATORY STUDY



Dimethyl fumarate ameliorates endotoxin-induced acute kidney injury against macrophage oxidative stress

Kejun Zhou^{a*}, Mengyi Xie^{b*}, Shuli Yi^c, Yun Tang^c, Haojun Luo^c, Qiong Xiao^c, Jun Xiao^d and Yi Li^c

^aDepartment of Pediatric Surgery, Hepatobiliary Research Institute, Affiliated Hospital of North Sichuan Medical College, Nanchong, China; ^bHepatobiliary Research Institute, Affiliated Hospital of North Sichuan Medical College, Nanchong, China; ^cDepartment of Nephrology, Clinical Research Center of Kidney Disease in Sichuan Province, Clinical Immunology Translational Medicine Key Laboratory of Sichuan Province, Sichuan Provincial People's Hospital, Medicine of School, University of Electronic Science and Technology of China, Chengdu, China; ^dDepartment of Cardiovascular Medicine, Chongqing University Center Hospital, Chongqing, China

ABSTRACT

Background: Characterized by macrophage infiltration, renal inflammation during septic acute kidney injury (AKI) reveals a ubiquitous human health problem. Unfortunately, effective therapies with limited side effects are still lacking. This study is aiming to elucidate the role of Dimethyl fumarate (DMF) in macrophages against oxidative stress of septic AKI.

Methods: Balb/c mice were gavaged by 50 mg/kg DMF then injected with 10 mg/kg LPS by *i.p.* We examined LPS-induced renal dysfunction and histological features in murine kidneys. Raw264.7 macrophage cells were also treated with DMF and then induced by LPS. The mitochondrion staining was used to follow mitochondria integrity by confocal microscopy. Flow cytometry measured the production of ROS by DCF-HDA and the expression of iNOS. Western blot detected the expression of Nrf-2 and Sirt1. Co-IP measured the interaction between Sirt1 and Nrf-2. Confocal microscopy observed the colocalization of Sirt1 and Nrf-2 in LPS-treated Raw264.7 macrophage cells.

Results: DMF ameliorated murine LPS nephritis with reduced blood urea nitrogen and serum creatinine, as well as decreased the histological alterations compared to the normal control. DMF significantly inhibited the expression of iNOS and reduced the production of nitrite in Raw264.7 cells following LPS treatment. Our study also revealed the role of DMF in protecting against intracellular ROS accumulation and mitochondria dysfunction in LPS-induced nephritis. DMF facilitated colocalization and interaction between Sirt1 and Nrf-2 in LPS-treated cells.

Conclusions: This study showed that DMF alleviated LPS-induced nephritis, indicating protective effects of DMF on macrophage against oxidative stress induced by LPS potentially involving Nrf-2-mediated pathway.

ARTICLE HISTORY

Received 2 December 2020
Revised 23 June 2021
Accepted 24 July 2021

KEYWORDS





Dimethyl fumarate;
macrophage; oxidative
stress; acute kidney injury

Introduction

Sepsis involving acute kidney injury (AKI) is the statistically leading cause of mortality in general ICU patients [1,2]. Since there is no effective therapy with limited side effects for septic AKI, it still remains a great challenge for both scientists and clinicians to control this disease [3]. Regarded as a major feature of pathogenesis, continued activation of macrophages may contribute to intensified septic response [4].

Macrophage malfunction is closely associated with the degree of renal structural injury and kidney

dysfunction in human renal diseases, such as rhabdomyolysis-induced kidney injury, polycystic kidney disease, and diabetic renal injury [5–7]. In the pathological process, macrophages have been considered as the crucial immune cells for their ability to display diverse functional phenotypes to respond for different microenvironments [8]. There are at least two phenotypically and functionally distinct subsets for macrophage polarization: classically activated M1 macrophages and alternatively activated M2 macrophages [9]. The regulation of the balance of pro-inflammatory M1 macrophages

CONTACT Yi Li  liyisn@med.uestc.edu.cn  Department of Nephrology, Clinical Research Center of Kidney Disease in Sichuan Province, Clinical Immunology Translational Medicine Key Laboratory of Sichuan Province, Sichuan Provincial People's Hospital, Medicine of School, University of Electronic Science and Technology of China, Chengdu, China; Jun Xiao  xj73wy@163.com  Department of Cardiovascular Medicine, Chongqing University Center Hospital, No. 1, Jiankang Road, YuZhong District, Chongqing, 400014, China.

*Zhou Kejun and Xie Mengyi contributed equally as the first author to this work.

© 2021 The Author(s). Published by Informa UK Limited, trading as Taylor & Francis Group.

This is an Open Access article distributed under the terms of the Creative Commons Attribution-NonCommercial License (<http://creativecommons.org/licenses/by-nc/4.0/>), which permits unrestricted non-commercial use, distribution, and reproduction in any medium, provided the original work is properly cited.

and anti-inflammatory M2 macrophages is an attractive target for attenuating the renal injury in numerous inflammatory pathophysiological conditions.

Dimethyl fumarate (DMF) is a methyl ester which owns some fascinating immuno-modulatory properties. In 2012, a slow release formulation of DMF was approved for its treatment to multiple sclerosis [10]. As a small therapeutic molecule for multiple sclerosis, DMF can activate cellular antioxidant signaling pathways through Nuclear factor erythroid 2-related factor 2 (Nrf-2) [11]. While oral DMF was proved to be effective for glucocorticoid-resistant lupus nephritis by involving Nrf-2 [12], the immuno-modulatory role and mechanism of DMF in septic AKI is still unclear.

To elucidate the unclear mechanism of septic AKI and further to find its independent risk for adverse outcome, this study examined the role of DMF in macrophage against oxidative stress of endotoxin-induced AKI. Our findings might be useful for designing potential clinical trials to prevent and treat septic AKI in critically ill patients.

Materials and methods

Reagents and chemicals

Dimethyl fumarate was obtained from Sigma-Aldrich company (#50744, Sigma-Aldrich, St. Louis, USA). Tween-20 (#P1379), LPS from *Escherichia coli* 0111:B4 (#L2690), Nrf-2 agonist Sulforaphane (#S6317) and ROS inhibitor NAC (#1009005) were also from Sigma.

Establish murine LPS nephritis model

Six to eight week-old female Balb/c mice were purchased from the Western China Experimental Animal Center of Sichuan University. According to National Institutes of Health Guidelines in China, all the mice were treated with human care and kept under temperature controlled conditions. LPS was dissolved in saline and *i.p.* injected the mice at a dosage of 10 mg/kg. According to previous study of Hsu CN and Jing et al. [13,14], we use 50 mg/kg DMF to treat the mice. Mice were weighed and randomly assigned to four groups: normal control group, LPS nephritis group, LPS + DMF group and DMF alone group ($n = 5$ per group). DMF was freshly prepared in 0.5% Tween-20/PBS. Control animals received 0.5% Tween-20/PBS as vehicle alone at the same frequency and volume as DMF. For DMF treatment, 50 mg/kg DMF was gavaged 30 min after LPS injection. Mice were sacrificed after anesthesia by 1.5% pentobarbital sodium *i.p.* following by LPS injection. Then the serum and kidney tissues were collected.

Cells

The murine macrophage cell line Raw264.7 (#SC-6003, Cryosite, Lane Cove, NSW, Australia) was purchased from the global Bioresource center ATCC. According to the supplier's instruction, the cells were cultured in DMEM with 10% FBS, 100 units/ml penicillin and 100 μ g/ml streptomycin. Cells were grown under an atmosphere condition of 95% air and 5% CO₂ at 37 °C.

Assessment of renal function

Blood samples were collected at 24 h after LPS injection. The levels of blood urea nitrogen (BUN) and serum creatinine (CREA) were detected by Creatinine (Cr) Assay kit (C011-2-1, Nanjing Jiancheng Biotech., Nanjing, China) with sarcosine oxidase method and Urea Assay Kit (C013-2-1, Nanjing Jiancheng Biotech.) with urease method.

Histology and immunohistochemistry

To assess renal injury under optical microscope, murine kidney sections were fixed in 10% formalin, embedded in paraffin, cut into 2- μ m sections and stained with hematoxylin-eosin. The dewaxed and hydrated 2- μ m renal tissue sections were incubated with 3% H₂O₂ for 10 min. After washed by PBS for three times, the sections were blocked with 5% BSA (BP9706100, Thermofisher Scientific, USA). The incubated the sections over night with primary antibodies against CD68 (1:200, #ab955, Abcam, Massachusetts, USA), and iNOS (1:100, #ab15323, Abcam). The sections were then washed by PBS for three times and stained using the Polink-2 plus Polymer HRP Detection System (#PV-9001/9002, ZSGB-Bio, Beijing, China). The result of PAS staining indicating damage score was interpreted by two pathological technicians who were doubleblinded. According to previous study by Zhang J, the damage score means: "0"=no damage, "1"=mild damage, "2"=moderate damage and "3"=severe damage [15].

Nitrite assay

Raw264.7 cells were seeded at 2×10^4 cells/well in 96-well plates (Costar Corning, Rochester, NY) and incubated in the culture medium overnight. The cells were pre-treated with various concentrations of DMF (0, 1.25, 2.5, 5, 10, 20 and 40 μ M) for 5 h and then respectively treated with 1 μ g/ml LPS for 24, 48 and 72 h. The nitrite accumulation in the supernatant was detected by the Griess reaction kit (#S0021, Beyotime, Shanghai, China). Mixed 50 μ l cell supernatant with an equal volume of Griess reagent

and incubated at room temperature for 10 min. The absorbance at 530 nm was measured by the Fluoroskan Ascent FI (ThermoFisher, USA). A series of known concentrations of sodium nitrite was used as standards.

Reactive oxygen species assay

Raw264.7 cells were seeded at 2×10^5 cells/well in 6-well plates (Costar Corning, Rochester, NY) and incubated in the culture medium overnight. The cells were respectively pretreated with $5 \mu\text{M}$ DMF and $5 \mu\text{M}$ SFN 5 h before $1 \mu\text{g/ml}$ LPS induction for 24 h. DCFH-DA (#S0033, Beyotime) was used to detect the ROS production of Raw264.7 cells. The intracellular reactive oxygen species could oxidize the non-fluorescent DCFH to be green fluorescent DCF. The fluorescence color change of DCF indicates the level of intracellular reactive oxygen species. Flow cytometric data for reactive oxygen assay were acquired using a Novocyte flow cytometer (ACEA Biosciences) at an excitation of 488 nm and an emission of 530 nm.

Mitotracker staining

To observe the cell morphology, Raw264.7 cells were pretreated with $5 \mu\text{M}$ DMF for 5 h and treated with $1 \mu\text{g/ml}$ LPS for 24 h. Normal saline was used as the normal control. The cells were incubated with 100 mM Mitotracker Red FM (#M22426, Invitrogen, USA) for 40 min at 37°C . The cells were then washed with PBS for three times, stained with DAPI (#M62248, Invitrogen, USA) for 5 min and washed again with PBS for three times. Images were captured by a confocal microscope (Leica MicroImaging, Leica TCS SP8, Germany) and processed by software provided by the manufacturer.

Confocal microscopy

For immunostaining, Raw264.7 cells were seeded at 2×10^5 cells/well in 6-well plates (Costar Corning, Rochester, NY). The cells were respectively pretreated with $5 \mu\text{M}$ or $10 \mu\text{M}$ DMF before 24 h LPS induction. The cells were fixed with 4% paraformaldehyde, permeabilized with 0.25% Triton-X 100, and washed with PBS. The cells were then incubated with rabbit polyclonal antibody against Nrf-2 (1:100, #ab31163, Abcam) or rabbit polyclonal antibody against Sirt1 (1:100, #13161-1-AP, Proteintech) at 4°C overnight. The cells were next washed with PBS for three times and incubated with Alexa Fluor 488 goat anti-rabbit IgG (1:1000, #ab150077, Abcam) for 1 h. DAPI (#M62248, Invitrogen, USA) was used to stain nuclei at the concentration of $1 \mu\text{M}$ and the

cells were washed with PBS for three times. The images were captured by a fluorescence confocal microscope (Leica MicroImaging, Leica TCS SP8, Germany) and processed by the manufacturer's software.

Western blot

Total protein of Raw264.7 cells was extracted by a RIPA lysis buffer (#P0013B, Beyotime). The protein concentrations were determined by the BCA Protein Assay kit (BioRad, Hercules, CA). The protein was stored at -80°C for western blotting analysis. The protein was mixed with $5 \times$ loading buffer and boiled at 100°C for 5 min, separated with 10% sodium dodecyl sulfate polyacrylamide gelelectrophoresis (SDS-PAGE) and transferred to PVDF membranes (ThermoFisher) at 100 V for 90 min. The membranes were blocked with 5% skim milk for 1 h and incubated with primary antibody against Nrf-2 (1:600, #16396-1-AP, Proteintech) and GAPDH (1:10000, #9295, Sigma), respectively at 4°C overnight. After washed by TBST for three times, the membranes were incubated with HRP conjugated goat anti-rabbit antibody (1:5000, #SA00001-2, Proteintech) at 37°C for 1 h. Then membranes were washed with TBST for three times and the signals were detected by an enhanced chemiluminescence detection kit (Millipore, USA). Image was captured by the ImageQuant LAS 4000 mini system (GE, USA).

Immunoblotting and immunoprecipitation

Raw264.7 cells were seeded at 5×10^6 cells/plate in 10 cm^2 plates and pretreated with $10 \mu\text{M}$ DMF before 24 h LPS induction. Total proteins of the cells were extracted by an IP lysis buffer (#P0013J, Beyotime). Protein concentrations were determined by the BCA Protein Assay kit (BioRad). The lysates were mixed with anti-Nrf-2 antibody (1:50, #12791, CellSignalingTechnology, USA) or anti-Sirt1 antibody (1:50, #13161-1-AP, Proteintech), which were coupled to agarose beads (Invitrogen). Immunoprecipitates were separated by SDS-PAGE and transferred to PVDF membranes. The membranes were respectively incubated with primary antibody against Sirt1 (1:600, #13161-1-AP, Proteintech) or antibody against Nrf-2 (1:1000, #12791, CellSignalingTechnology), and washed by TBST. Then the membranes were incubated with HRP conjugated goat anti-rabbit antibody (1:5000, #SA00001-2, Proteintech) and the signal was detected by an enhanced chemiluminescence detection kit (Millipore, USA). Results were obtained by the ImageQuant LAS 4000 mini system (GE, USA).

Statistical analysis

Data were shown by ratios or percentages compared with normal controls \pm SD from three independent experiments. Parametric data were statistically analyzed by one-way ANOVA. $p < 0.05$ indicated a statistically significant difference. Statistical analysis was performed by the SPSS (Version 13.0, SPSS Inc., Chicago, IL).

Results

DMF ameliorated LPS induced renal dysfunction in mice

To observe the effect of DMF on renal dysfunction during LPS nephritis, we detected the BUN and CREA of murine blood samples at the time point of 24 h post LPS injection. At 24 h, the level of CREA in LPS nephritis group increased to $38.20 \pm 6.44 \mu\text{M}$, compared to $9.43 \pm 2.86 \mu\text{M}$ in the normal control group and $11.24 \pm 1.56 \mu\text{M}$ in the DMF alone group. However, 50 mg/kg DMF pre-administration significantly reduced the level of CREA to $13.97 \pm 4.30 \mu\text{M}$ at 24 h, which all significantly reduced compared to those of LPS nephritis group (Figure 1(A)). BUN in mice of the LPS nephritis group exhibited a significant increase to $34.38 \pm 5.19 \mu\text{M}$ at 24 h following LPS injection, compared to $4.83 \pm 1.10 \mu\text{M}$ in normal control group and $6.48 \pm 0.83 \mu\text{M}$ in the DMF alone group. However, 50 mg/kg DMF administration after LPS injection significantly reduced the level of BUN to $12.70 \pm 2.45 \mu\text{M}$ (Figure 1(B)). The results indicated that DMF was effective for protecting mice against renal dysfunction induced by LPS.

DMF treatment attenuated histological changes in endotoxin-induced acute kidney injury

To further elucidate the role of DMF in LPS stimulated nephritis, we observed the histological changes upon DMF treatment of murine LPS nephritis. Light microscopy about Hematoxylin & eosin (H & E) staining and Periodic Acid-Schiff (PAS) staining showed that LPS injection induced severe renal pathological lesions, including impaired brush border of renal tubule, damaged renal tubular epithelial cells and infiltration of inflammatory cells, compared to normal control mice. In contrast, DMF treatment followed by LPS injection reduced the pathological features in murine kidney (Figure 2(A)). LPS injection could significantly increase the damage score in murine kidney indicating severe renal injury. However, DMF treatment could reduce the

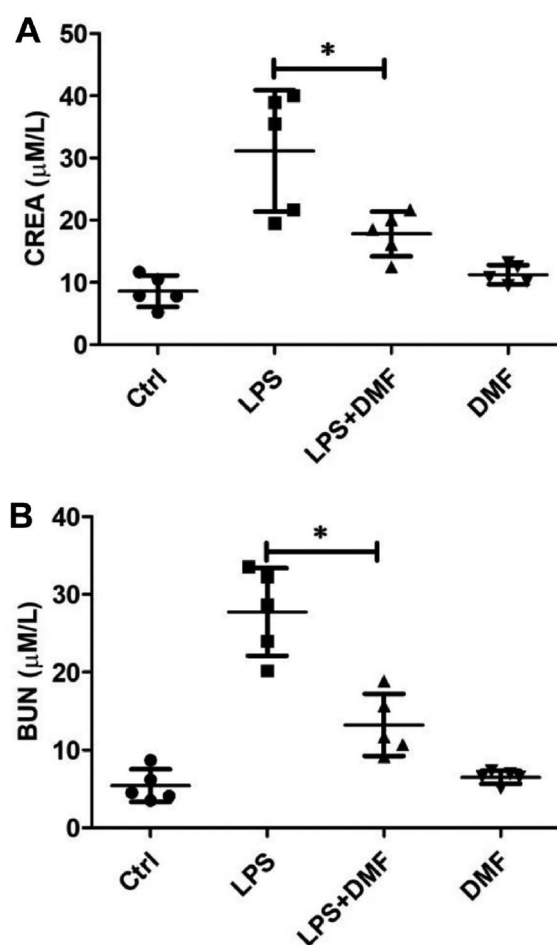


Figure 1. DMF ameliorated LPS-induced renal dysfunction in mice. The BUN and CREA of murine blood samples were detected at 24 h post LPS injection. LPS was dissolved in saline and *i.p.* injected the mice at a dosage of 10 mg/kg. Mice were weighed and randomly assigned to four groups: normal control group, LPS nephritis group, LPS + DMF group and LPS + DMF alone group ($n = 5$ per group). DMF was freshly prepared in 0.5% Tween-20/PBS. Control animals received 0.5% Tween-20/PBS as vehicle alone at the same frequency and volume as DMF. For DMF treatment, 50 mg/kg DMF was gavaged 30 min after LPS injection. Blood samples were collected at 24 h after LPS injection. (A) CREA levels of murine blood samples collected at 24 h post LPS injection. (B) BUN levels of murine blood samples collected at 24 h post LPS injection. Statistically significant differences are indicated by $*p < 0.05$ or $**p < 0.01$. DMF: dimethyl fumarate; CREA: serum creatinine; BUN: blood urea nitrogen.

damage score in mice kidney suggesting potential role of DMF against renal injury (Figure 2(B)).

DMF inhibited the expression of CD68 and iNOS mice kidney after LPS injection and production of nitrite in LPS-induced macrophages

To analyze the effect of DMF on infiltrated inflammatory cells in LPS-induced nephritis, we performed

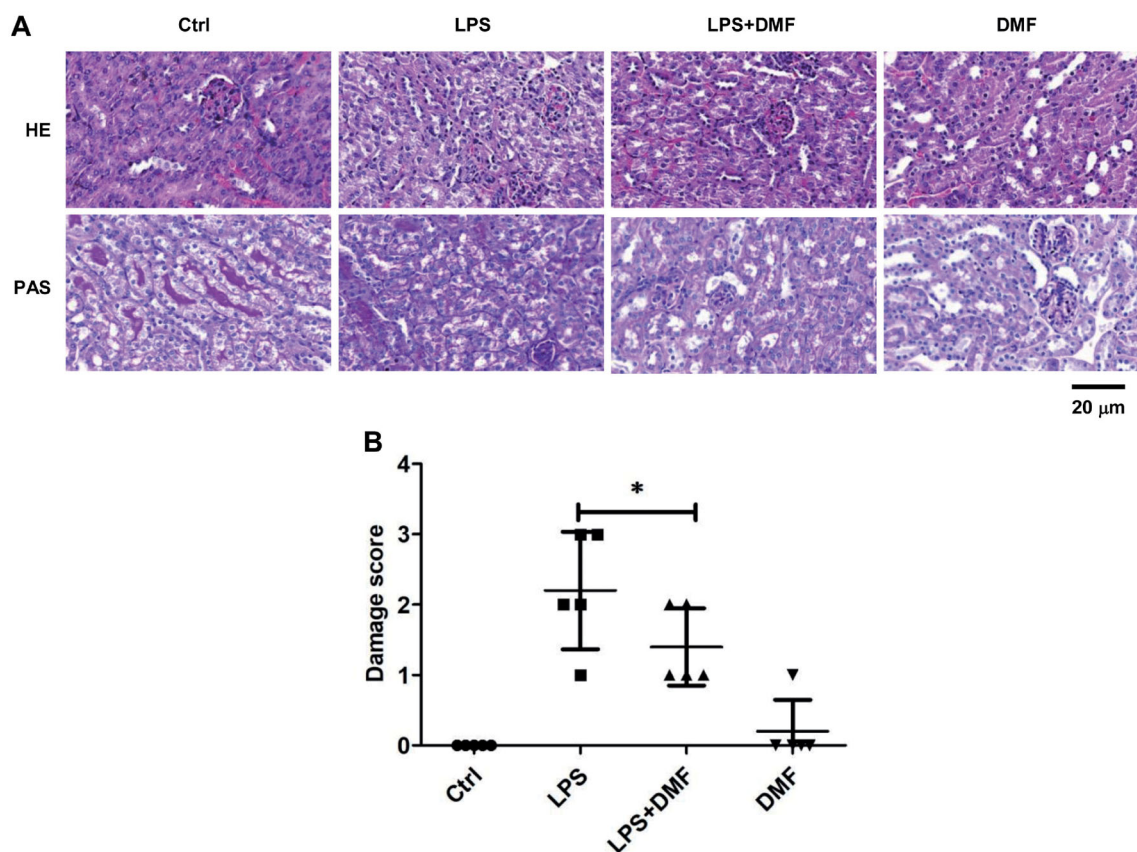


Figure 2. DMF treatment attenuated histological alterations in LPS-induced nephritis. To assess renal injury under optical microscope, murine kidney sections were fixed in 10% formalin, embedded in paraffin and cut into 2- μ m sections. (A) H&E staining and PAS staining. Images are shown at a magnification of 20 μ m. (B) Damage score based on PAS staining. Statistically significant differences are indicated by $*p < 0.05$. DMF: dimethyl fumarate.

immunohistological staining of CD68 and iNOS. In addition, kidneys of mice in DMF treated group had markedly less CD68⁺ cell infiltration than mice without DMF treatment. iNOS⁺ cell infiltration was reduced in mice of DMF treatment compared to mice of the LPS injection group. The results showed that DMF treatment might attenuate histological damages and decreased the expression of CD68 and iNOS in mice kidney after LPS injection (Figure 3(A)). We also determined the production of nitric oxide in the supernatant of LPS-induced Raw264.7 macrophage cells by testing the amount of nitrite, a stable metabolite of nitric oxide [16]. The cells produced $5.06 \pm 1.51 \mu\text{M}$ nitrite in normal control group. LPS induction for 24 h increased the secretion of nitrite to $7.11 \pm 0.13 \mu\text{M}$, whereas nitrite secretion was reduced to $6.74 \pm 0.11 \mu\text{M}$ and $6.62 \pm 0.18 \mu\text{M}$ by 5 μM and 10 μM (DMF), respectively (Figure 3(B)). Compared with $5.87 \pm 2.14 \mu\text{M}$ nitrite in normal control group, LPS induction for 48 h increased the secretion of nitrite to $9.75 \pm 0.11 \mu\text{M}$, whereas nitrite secretion was reduced to $8.68 \pm 0.07 \mu\text{M}$, $8.18 \pm 0.11 \mu\text{M}$, $7.26 \pm 0.18 \mu\text{M}$, $6.00 \pm 0.18 \mu\text{M}$, and $6.13 \pm 0.11 \mu\text{M}$ by

adding 5 μM , 10 μM , 20 μM and 40 μM DMF respectively (Figure 3(C)). Compared with $6.18 \pm 1.32 \mu\text{M}$ nitrite in normal control group, LPS induction for 72 h increased the secretion of nitrite to $10.35 \pm 0.48 \mu\text{M}$, whereas 2.5 μM DMF inhibited nitrite secretion to $8.31 \pm 0.07 \mu\text{M}$, 5 μM DMF inhibited nitrite secretion to $8.08 \pm 0.09 \mu\text{M}$, 10 μM DMF inhibited nitrite secretion to $7.21 \pm 0.13 \mu\text{M}$, 20 μM DMF inhibited nitrite secretion to $5.92 \pm 0.10 \mu\text{M}$ upon LPS stimulation and 40 μM DMF inhibited nitrite secretion to $4.85 \pm 0.06 \mu\text{M}$ upon LPS stimulation (Figure 3(D)). These findings suggested that DMF could inhibit production of Nitrite in LPS-induced macrophage in a time- and dosage-dependent manner.

DMF suppressed LPS-induced oxidative injury and mitochondria dysfunction of macrophages

Having confirmed the effective dosage of DMF for LPS stimulated Raw264.7 cells by Griess reagent, we observed that LPS increased the percentage of DCF⁺ cells to 99%, compared to 0.33% in normal control group, whereas 5 μM DMF decreased it to 81.46% and

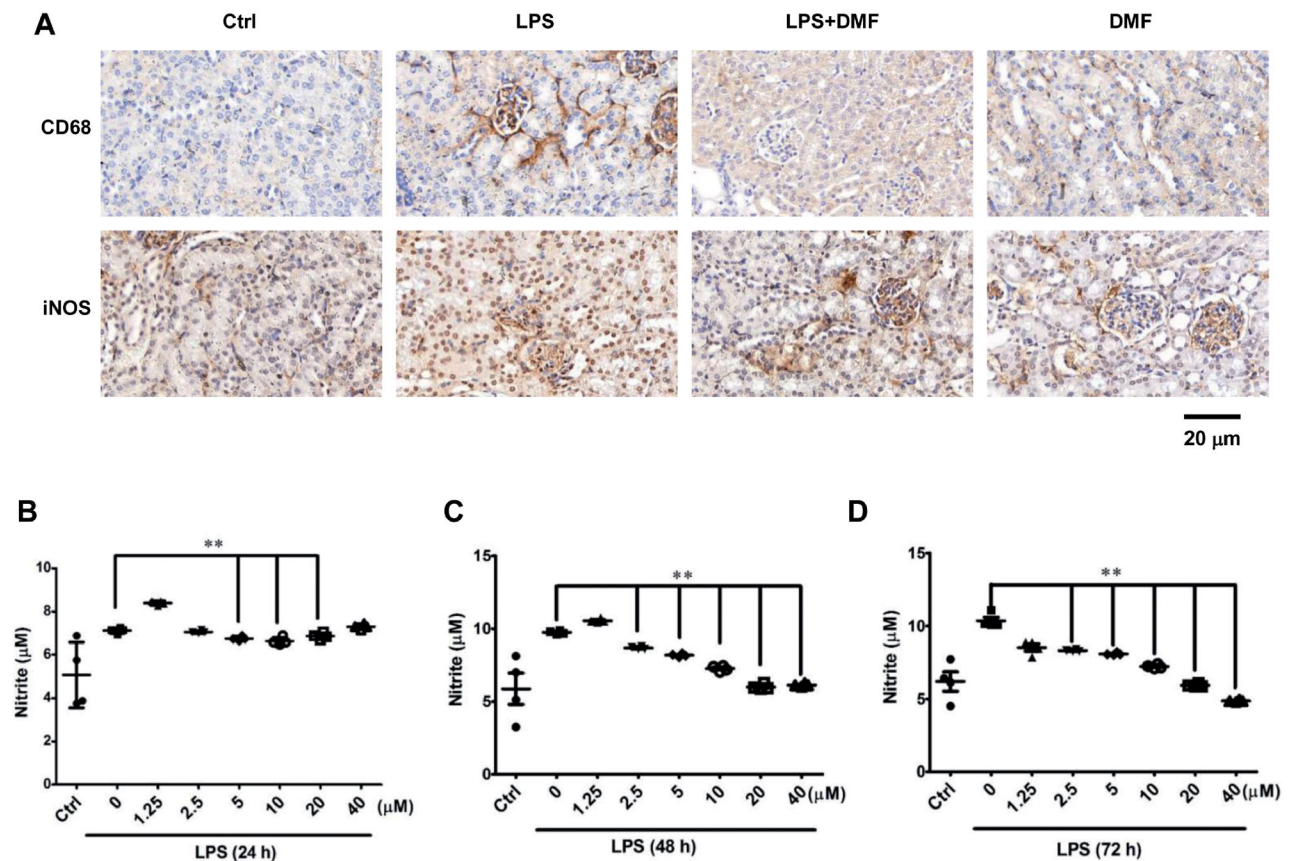


Figure 3. DMF inhibited the expression of CD68 and iNOS in mice kidney after LPS injection and production of Nitrite in LPS-induced macrophages. To assess renal injury under optical microscope, murine kidney sections were fixed in 10% formalin, embedded in paraffin, cut into 2- μm sections and stained with immunohistological staining. Raw264.7 cells were seeded at 2×10^4 cells/well in 96-well plates and incubated in the culture medium overnight. The cells were pretreated with various concentrations of DMF (0, 1.25, 2.5, 5, 10, 20 and 40 μM) for 5 h and then respectively treated with 1 $\mu\text{g}/\text{ml}$ LPS for 24, 48 and 72 h. The nitrite accumulation in the supernatant was detected by the Griess reagent. (A) Immunohistological staining of CD68 and iNOS. Images are shown at a magnification of 20 μm . (B) Production of Nitrite in LPS-stimulated macrophages at 24 h. (C) Production of Nitrite in LPS-stimulated macrophages at 48 h. (D) Production of Nitrite in LPS-stimulated macrophages at 72 h. Statistically significant differences are indicated by $**p < 0.01$. DMF: dimethyl fumarate.

5 μM SFN decreased it to 94.09% (Figure 4(A)). These showed that DMF might suppress LPS-induced oxidative injury of macrophages. After incubated the cells with Mitotracker Red FM, we found that exposure to 1 $\mu\text{g}/\text{ml}$ LPS for 24 h greatly impaired the mitochondrial function reflected by reduction in the red fluorescent intensity when compared to normal control cells. However, 5 μM DMF significantly increased the red fluorescent intensity in Raw264.7 cells upon LPS stimulation (Figure 4(B)). It showed that DMF might suppress LPS-induced mitochondria dysfunction in macrophages.

DMF activated Nrf-2 translocation in LPS-stimulated Raw264.7 cells

In *in vitro* analysis, we observed that LPS induction reduced the protein level of Nrf-2 in nuclear of macrophages. DMF could significantly increase the nuclear

protein level of Nrf-2 in macrophages after LPS stimulation (Figure 5(A)). DMF could also significantly increase the expression of Nrf-2 in cytoplasm of macrophages after LPS stimulation (Figure 5(A)). Confocal microcopies showed that LPS significantly reduced Nrf-2 expression in the nuclei and increased Nrf-2 expression in the cytoplasm, compared with that of normal control group. However, DMF increased Nrf-2 expression in the nuclei and decreased Nrf-2 expression in the cytoplasm (Figure 5(B)).

DMF induced potential colocalization between Sirt1 and Nrf-2 after LPS stimulation

In *in vivo* study, we observed that LPS reduced the expression of Sirt1 and Nrf-2 in murine kidney tissue, whereas DMF could increase the expression expression of Sirt1 and Nrf-2 in murine kidney tissue after LPS

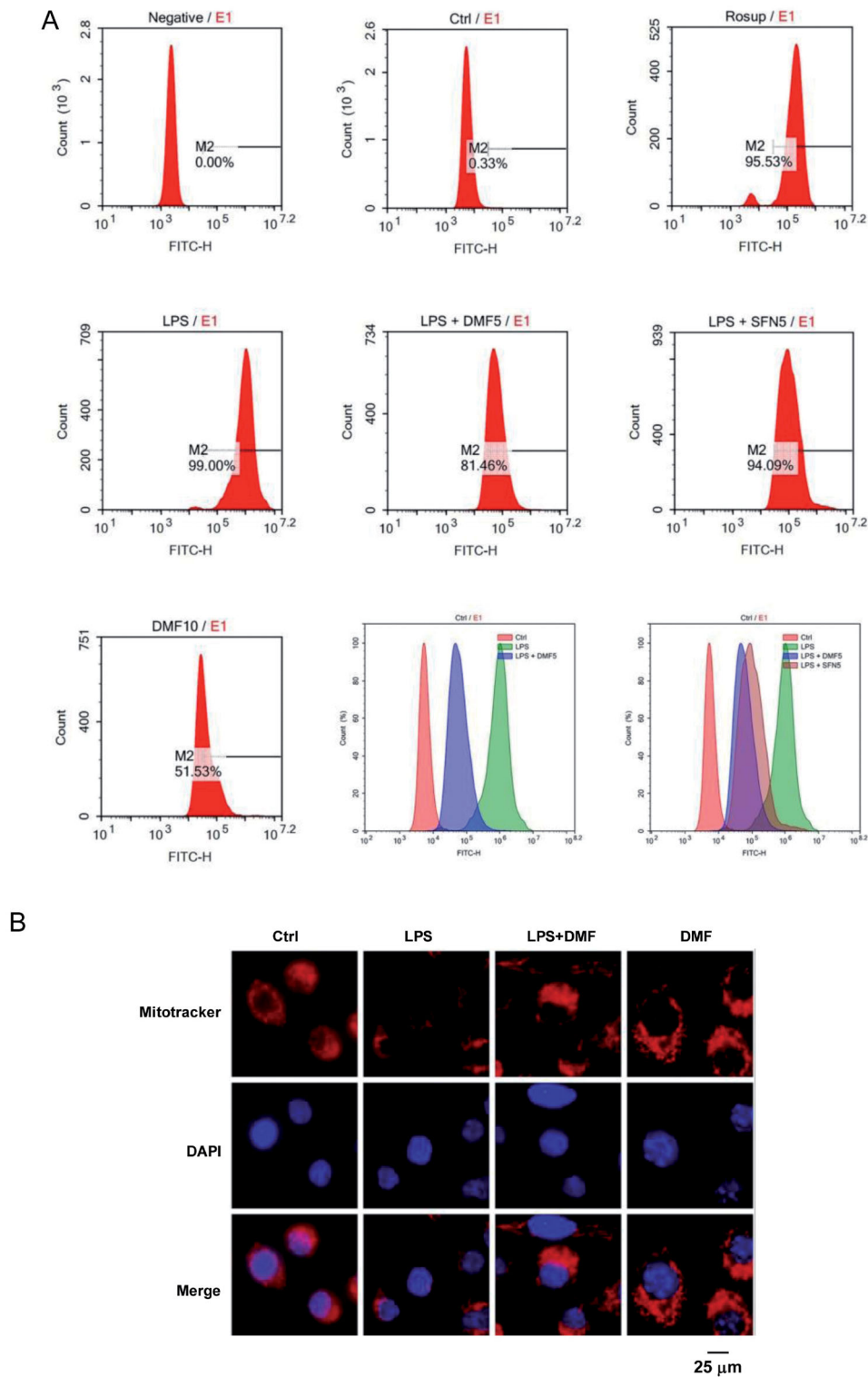


Figure 4. DMF suppressed LPS-induced oxidative injury and mitochondria dysfunction of macrophages. Raw264.7 cells were seeded at 2×10^5 cells/well in 6-well plates and incubated in the culture medium overnight. The cells were respectively pre-treated with 5μ M DMF and 5μ M SFN 5 h before 1μ g/ml LPS induction for 24 h. DCFH-DA was used to detect the ROS production of Raw264.7 cells by flow cytometry. Flow cytometric data for reactive oxygen assay were acquired using a Novocyte flow cytometer at an excitation of 488 nm and an emission of 530 nm. (A) Flowcytometry detection of DCFH-DA. (B) Confocal images observed by Mitotracker Red FM. Images are shown at a magnification of 25μ m. DMF: dimethyl fumarate; SFN: Sulforaphane.

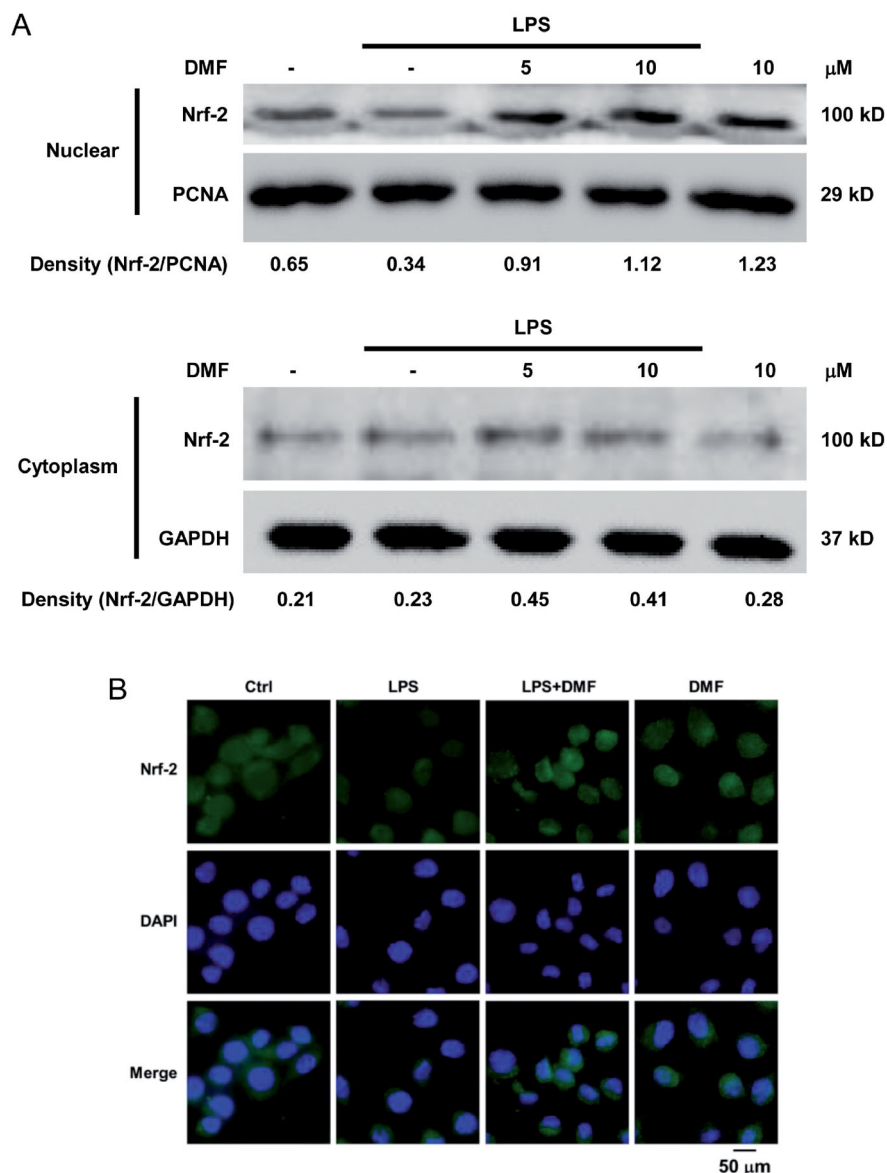


Figure 5. DMF activated Nrf-2 translocation in LPS-stimulated Raw264.7 cells. Raw264.7 cells were seeded at 2×10^5 cells/well in 6-well plates and incubated in the culture medium overnight. The cells were respectively pretreated with $5 \mu\text{M}$ DMF hours before $1 \mu\text{g/ml}$ LPS induction for 24 h. (A) Western blot detected the expression of Nrf-2 in the nuclear and cytoplasm of Raw264.7 cells. (B) Confocal observation of Nrf-2 in Raw264.7 cells. Images are shown at a magnification of $50 \mu\text{m}$. DMF: dimethyl fumarate.

injection (Figure 6(A)). Then we found there was an interaction between Sirt1 and Nrf-2 in Raw264.7 macrophages after DMF treatment (Figure 6(B)). We also found that LPS impaired the colocalization of Sirt1 and Nrf-2 in Raw264.7 cells by fluorescence confocal microscopy, whereas DMF promoted the colocalization of Sirt1 and Nrf-2 in LPS-treated cells (Figure 6(C)).

Discussion

Septic AKI is a major cause for the death of critically ill patients worldwide [17]. Characterized by macrophage infiltration, renal inflammation in septic AKI represents

a ubiquitous human health problem, but effective therapies with limited side effects are still lacking [18]. In this study, we observed DMF could attenuate renal dysfunction and pathological damage in mice with LPS-induced AKI. DMF treatment decreased the expression of CD68 and iNOS in mice kidney after LPS injection, indicating the potential role of DMF in macrophage oxidative stress. Then current study aimed to elucidate the potential role of DMF in LPS-induced acute kidney injury against oxidative stress of macrophages.

Previous mechanistic studies suggested that the therapeutic mechanism of DMF is mainly involved in Nrf-2-dependent regulation of oxidative stress [19,20].

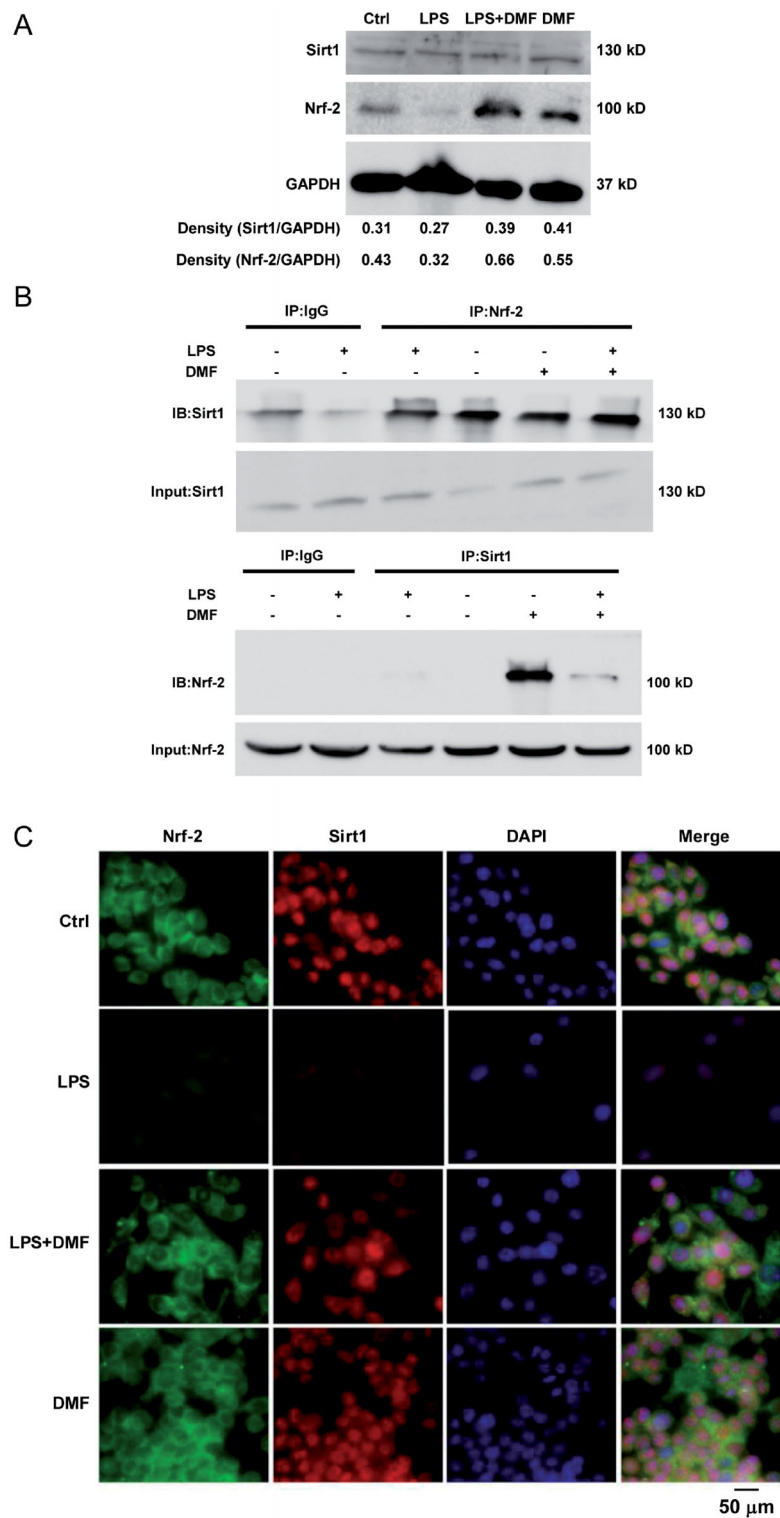


Figure 6. DMF induced potential colocalization between Sirt1 and Nrf-2 after LPS stimulation. LPS was dissolved in saline and *i.p.* injected the mice at a dosage of 10 mg/kg. Mice were weighed and randomly assigned to four groups: normal control group, LPS nephritis group, LPS + DMF group and LPS + DMF alone group ($n = 5$ per group). DMF was freshly prepared in 0.5% Tween-20/PBS. Control animals received 0.5% Tween-20/PBS as vehicle alone at the same frequency and volume as DMF. For DMF treatment, 50 mg/kg DMF was gavaged 30 min after LPS injection. Blood samples were collected at 24 h after LPS injection. Raw264.7 cells were seeded at 5×10^6 cells/plate in 10 cm^2 plates for Co-IP and 2×10^5 cells/well in 6-well plates for immunostaining with confocal. Then the cells were incubated in the culture medium overnight. The cells were pretreated with $5 \mu\text{M}$ DMF hours before $1 \mu\text{g/ml}$ LPS induction for 24 h. (A) Western blot detected the expression of Nrf-2 and Sirt1 in murine renal tissue after LPS injection. (B) Co-IP between Nrf-2 and Sirt1 in Raw264.7 cells after DMF treatment. (C) Confocal observed colocalization between Sirt1 and Nrf-2 after DMF treatment. Images are shown at a magnification of $50 \mu\text{m}$. DMF: dimethyl fumarate.

A series of evidence have shown that Nrf-2 is beneficial for autoimmune disorders and inflammatory diseases, such as multiple sclerosis and neurodegenerative diseases [21,22]. Activation of Nrf-2 could protect cells from apoptosis and inflammation through regulation of oxidative stress [23]. Once activated by redundant ROS accumulation under oxidative stress, Nrf-2 could dissociate with Keap1 and translocate from the cytoplasm to the nuclei [24]. In our study, DMF increased the expression of Nrf-2 in nuclei of macrophages after LPS stimulation. It suggested that DMF activated Nrf-2 translocation in LPS-stimulated macrophages.

Nrf-2 pathway is an important antioxidant pathway against oxidative stress by removal of oxygen free radicals [25,26]. Correlated with the activated Nrf-2 translocation role of DMF, we observed that DMF suppressed LPS-induced oxidative injury and mitochondria dysfunction in macrophages. Wilms et al. have reported that DMF reduced the production of nitric oxide in brain inflammation [19]. Liu et al. reported that DMF suppressed iNOS activities in dextran sulfate sodium-induced murine experimental colitis [27]. In the current study, we also observed that DMF inhibited production of nitrite in LPS-treated macrophages at a time- and dose-dependent manner. These indicated the role of DMF in inhibition of oxidative stress in endotoxin-induced AKI.

Sirtuin 1 (Sirt1) is a NAD⁺-dependent deacetylase that exerts many pleiotropic effects of oxidative metabolism. He et al. observed that Sirt1 activation could protect murine renal medulla from oxidative injury [28]. Sirt1 is also known to induce the deacetylation of Nrf-2 that subsequently reduces Nrf-2-dependent gene transcription [29]. And we observed that DMF could increase the expression expression of Sirt1 and Nrf-2 in murine kidney tissue after LPS injection. DMF also induced potential colocalization between Sirt1 and Nrf-2 in LPS-stimulated Raw264.7 cells. These results indicate that DMF activated the interaction between Sirt1 and Nrf-2 in LPS-stimulated Raw264.7 cells to enhance defense against oxidative stress.

Due to limitation to current study, we just observed the potential role of DMF in LPS-induced AKI against oxidative stress of macrophages and did not precisely elucidate the mechanism of DMF in mitochondria oxidative stress of macrophages. Our further study will focus on the mechanism of DMF to understand how oxidative stress is specifically regulated in mitochondria. And for the importance of macrophage polarization in sepsis, we will study the role and mechanism of DMF in macrophage polarization in LPS-induced AKI in next.

Hence, our study revealed that DMF alleviated the outcome of LPS-induced AKI. In particular, it revealed protective effects of DMF on regulating macrophage against oxidative stress in LPS-induced acute renal inflammation potentially involving Nrf-2-mediated pathway.

Acknowledgements

Authors thank Prof. Deng Shaoping and Prof. Yang Zhenglin in University of Electronic Science and Technology, Sichuan Academy of Medical Sciences & Sichuan Provincial People's Hospital for generously providing research platforms and technical support.

Disclosure statement

Zhou Kejun, Xie Mengyi and Yi Shuli carried out the experimental work and the data collection and interpretation. Li Yi participated in the design and coordination of experimental work and acquisition of data. Tang Yun, Luo Haojun and Xiaoqiong participated in immunohistochemical studies. Xiao Jun and Li Yi carried out the study design and drafted the manuscript. The authors declare no financial or commercial conflict of interest.

Funding

This work was supported by National Natural Science Foundation of China [81700607 and 8170742], Fundamental Research Funds for the Central Universities from UESTC [ZYGX2019J105], Key R & D projects in Sichuan Province [2019YFS0538], The grant from Department of Science and Technology of Sichuan Province [2020ZYD034], The application foundation project of Sichuan Science and Technology Department [2018JY0332], The innovation project of medical research youth in Sichuan Province [Q16024 and Q16026] and The project from Nanchong science and Technology Bureau [200248].

References

- [1] Lee S, Kim W, Kang KP, et al. Agonist of peroxisome proliferator-activated receptor-gamma, rosiglitazone, reduces renal injury and dysfunction in a murine sepsis model. *Nephrol Dial Transplant*. 2005;20(6):1057–1065.
- [2] Vaara ST, Pettila V, Kaukonen KM, et al. The attributable mortality of acute kidney injury: a sequentially matched analysis*. *Crit Care Med*. 2014;42(4):878–885.
- [3] Costa NA, Gut AL, Azevedo PS, et al. Erythrocyte superoxide dismutase as a biomarker of septic acute kidney injury. *Ann Intensive Care*. 2016;6(1):95.
- [4] Dai M, Wu L, He Z, et al. Epoxyeicosatrienoic acids regulate macrophage polarization and prevent LPS-induced cardiac dysfunction. *J Cell Physiol*. 2015; 230(9):2108–2119.
- [5] Belliere J, Casemayou A, Ducasse L, et al. Specific macrophage subtypes influence the progression of

- Rhabdomyolysis-Induced kidney injury. *J Am Soc Nephrol.* 2015;26(6):1363–1377.
- [6] Swenson-Fields KI, Vivian CJ, Salah SM, et al. Macrophages promote polycystic kidney disease progression. *Kidney Int.* 2013;83(5):855–864.
- [7] You H, Gao T, Cooper TK, et al. Macrophages directly mediate diabetic renal injury. *Am J Physiol Renal Physiol.* 2013;305(12):F1719–F1727.
- [8] Gordon S, Taylor PR. Monocyte and macrophage heterogeneity. *Nat Rev Immunol.* 2005;5(12):953–964.
- [9] Ghosn EEB, Cassado AA, Govoni GR, et al. Two physically, functionally, and developmentally distinct peritoneal macrophage subsets. *Proc Natl Acad Sci USA.* 2010;107(6):2568–2573.
- [10] Limmroth V. Multiple sclerosis: oral BG12 for treatment of relapsing-remitting MS. *Nat Rev Neurol.* 2013;9(1):8–10.
- [11] Huang H, Tarabozetti A, Shriver LP. Dimethyl fumarate modulates antioxidant and lipid metabolism in oligodendrocytes. *Redox Biol.* 2015;5:169–175.
- [12] Ebihara S, Tajima H, Ono M. Nuclear factor erythroid 2-related factor 2 is a critical target for the treatment of glucocorticoid-resistant lupus nephritis. *Arthritis Res Ther.* 2016;18(1):139.
- [13] Hsu CN, Lin YJ, Yu HR, et al. Protection of male rat offspring against hypertension programmed by prenatal dexamethasone administration and postnatal High-Fat diet with the Nrf2 activator dimethyl fumarate during pregnancy. *Int J Mol Sci.* 2019;20(16):3957.
- [14] Jing X, Shi H, Zhang C, et al. Dimethyl fumarate attenuates 6-OHDA-induced neurotoxicity in SH-SY5Y cells and in animal model of parkinson's disease by enhancing Nrf2 activity. *Neuroscience.* 2015;286:131–140.
- [15] Zhang J, Zhang Y, Xiao F, et al. The peroxisome proliferator-activated receptor γ agonist pioglitazone prevents NF- κ B activation in cisplatin nephrotoxicity through the reduction of p65 acetylation via the AMPK-SIRT1/p300 pathway. *Biochem Pharmacol.* 2016;101:100–111.
- [16] Li Y, Wang ZL, He F, et al. TP-58, a novel thienopyridine derivative, protects mice from concanavalinA-induced hepatitis by suppressing inflammation. *Cell Physiol Biochem.* 2012;29(1–2):31–40.
- [17] Singbartl K, Kellum JA. AKI in the ICU: definition, epidemiology, risk stratification, and outcomes. *Kidney Int.* 2012;81(9):819–825.
- [18] Wang Y, Chang J, Yao B, et al. Proximal tubule-derived colony stimulating factor-1 mediates polarization of renal macrophages and dendritic cells, and recovery in acute kidney injury. *Kidney Int.* 2015;88(6):1274–1282.
- [19] Wilms H, Sievers J, Rickert U, et al. Dimethylfumarate inhibits microglial and astrocytic inflammation by suppressing the synthesis of nitric oxide, IL-1 β , TNF- α and IL-6 in an in-vitro model of brain inflammation. *J Neuroinflammation.* 2010;7(1):30.
- [20] Kume T, Suenaga A, Izumi Y, et al. Protective effect of dimethyl fumarate on an oxidative stress model induced by sodium nitroprusside in mice. *Biol Pharm Bull.* 2016;39(6):1055–1059.
- [21] Lee JM, Johnson JA. An important role of Nrf2-ARE pathway in the cellular defense mechanism. *J Biochem Mol Biol.* 2004;37(2):139–143.
- [22] Lee DH, Gold R, Linker RA. Mechanisms of oxidative damage in multiple sclerosis and neurodegenerative diseases: therapeutic modulation via fumaric acid esters. *Int J Mol Sci.* 2012;13(9):11783–11803.
- [23] Kensler TW, Wakabayashi N, Biswal S. Cell survival responses to environmental stresses via the Keap1-Nrf2-ARE pathway. *Annu Rev Pharmacol Toxicol.* 2007;47:89–116.
- [24] Itoh K, Wakabayashi N, Katoh Y, et al. Keap1 represses nuclear activation of antioxidant responsive elements by Nrf2 through binding to the amino-terminal Neh2 domain. *Genes Dev.* 1999;13(1):76–86.
- [25] Jeong WS, Jun M, Kong AN. Nrf2: a potential molecular target for cancer chemoprevention by natural compounds. *Antioxid Redox Signal.* 2006;8(1–2):99–106.
- [26] Chapple SJ, Siow RC, Mann GE. Crosstalk between Nrf2 and the proteasome: therapeutic potential of Nrf2 inducers in vascular disease and aging. *Int J Biochem Cell Biol.* 2012;44(8):1315–1320.
- [27] Liu X, Zhou W, Zhang X, et al. Dimethyl fumarate ameliorates dextran sulfate sodium-induced murine experimental colitis by activating Nrf2 and suppressing NLRP3 inflammasome activation. *Biochem Pharmacol.* 2016;112:37–49.
- [28] He W, Wang Y, Zhang MZ, et al. Sirt1 activation protects the mouse renal medulla from oxidative injury. *J Clin Invest.* 2010;120(4):1056–1068.
- [29] Kawai Y, Garduno L, Theodore M, et al. Acetylation-deacetylation of the transcription factor Nrf2 (nuclear factor erythroid 2-related factor 2) regulates its transcriptional activity and nucleocytoplasmic localization. *J Biol Chem.* 2011;286(9):7629–7640.